Supporting information

Figure S1

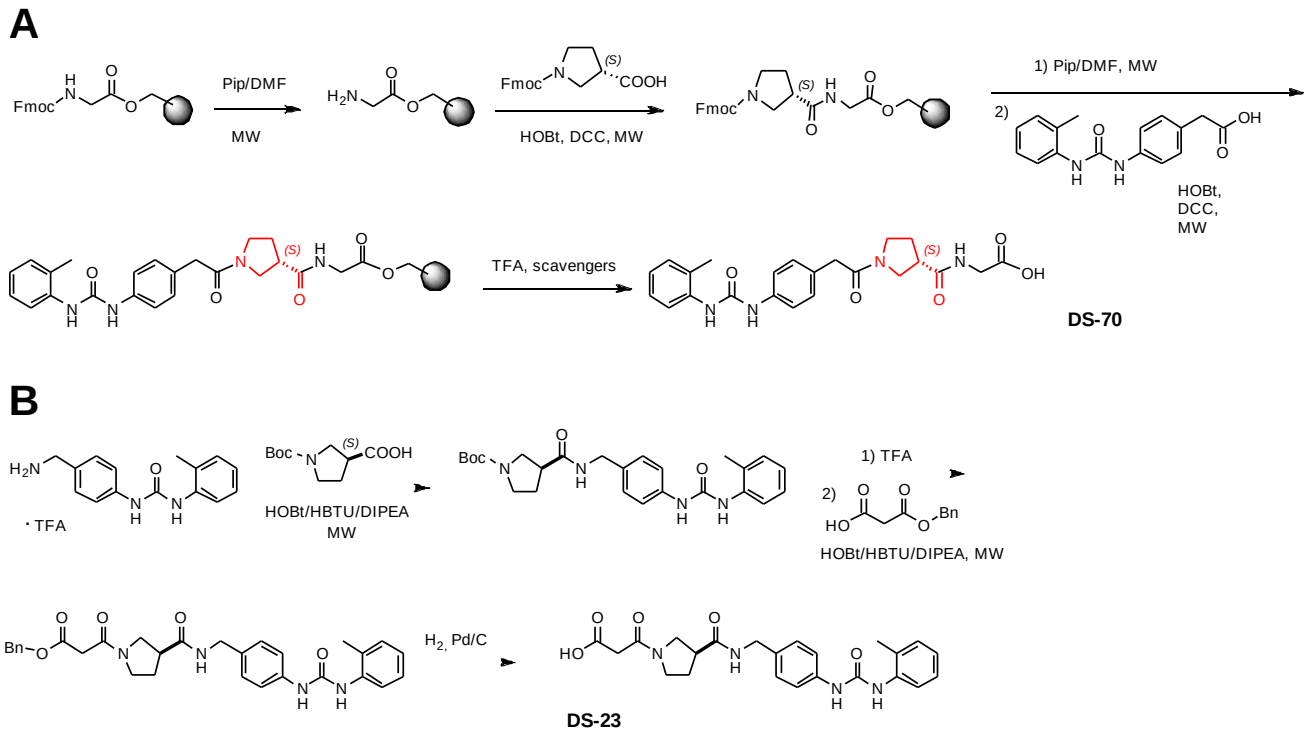

Figure S1

Relevant steps of the synthesis designed for DS-70 (A) and DS-23 (B) compounds, as described in the Methods.

Figure S2

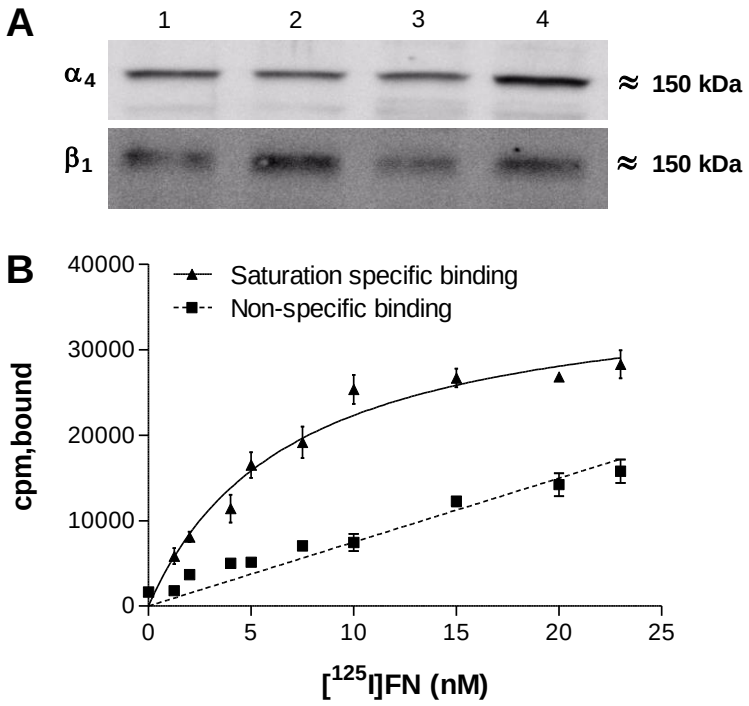

Figure S2

[^{125}I]-FN binds to the complex between $\alpha_4\beta_1$ integrin and the antibody anti-α_4 integrin in the presence of scintillation beads coated with an anti-rabbit IgG antibody (the procedure is described in the Methods). (A) Representative autoradiogram of a western blot experiment, evaluating, separately, α_4 and β_1 integrin subunits in cell lysate fractions (1 - 4) of Jurkat E6.1 cells, expressing $\alpha_4\beta_1$ integrin. Fractions 1- 4 were used in the SPA assays. (B) Saturation SPA binding of [^{125}I]-FN to $\alpha_4\beta_1$ integrin extracted and purified from Jurkat E6.1 cells and incubated with antibody anti-α_4 integrin, scintillation beads coated with the anti-rabbit IgG antibody and the radioligand. Non-specific binding was determined in the presence of increasing concentrations of [^{125}I]-FN (1-25 nM) and of 100 nM BIO1211. Saturation specific binding was determined by subtracting the non-specific binding from total binding counts. [^{125}I]-FN bound was expressed as counts per minute (cpm). Data are presented as mean ± SEM of five experiments in triplicate.

Figure S3

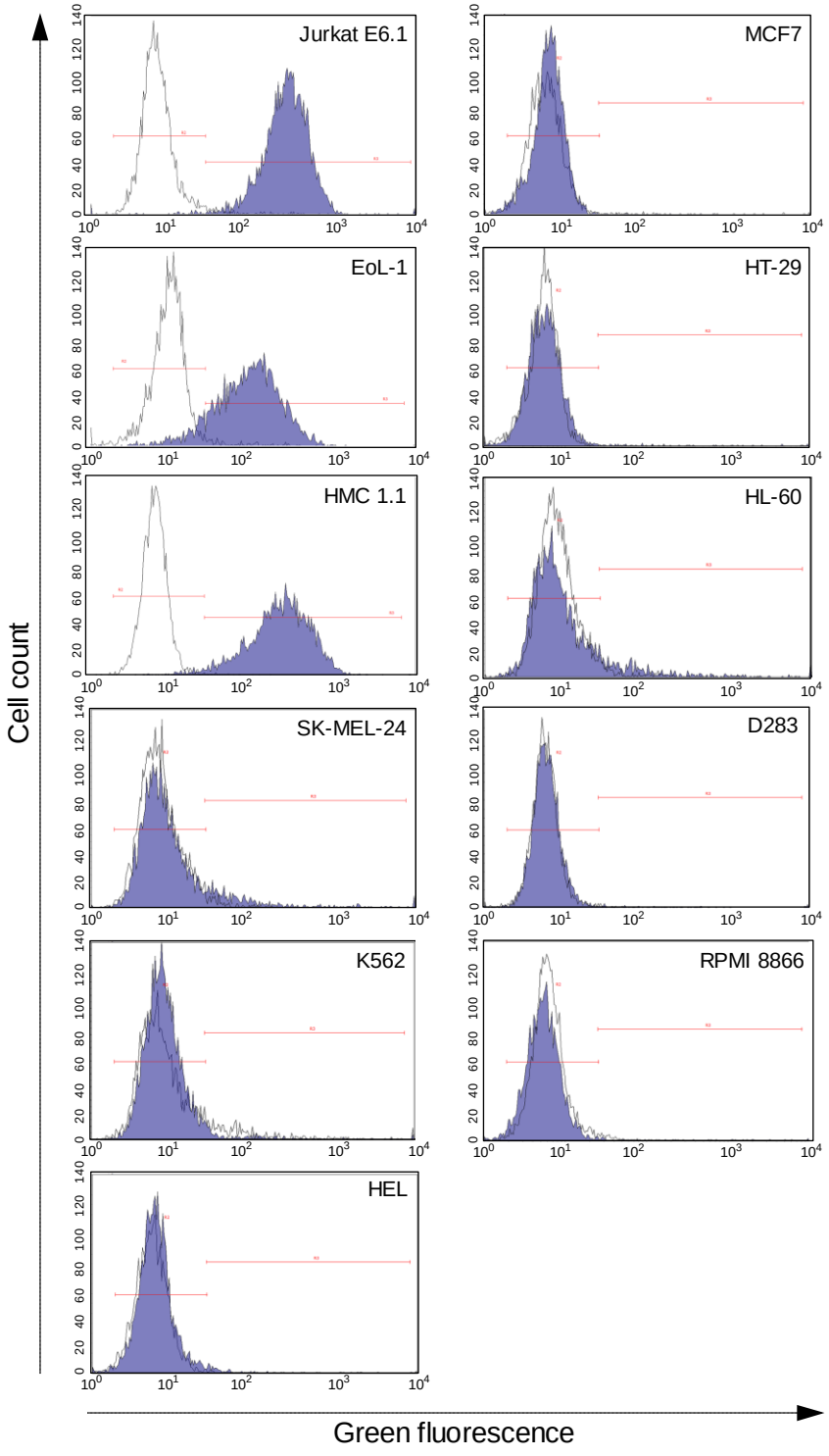

Figure S3

Flow cytometry plots (number of cells count *vs.* green fluorescence) showing relative surface expression of integrin α_4 (filled peak) on all cell lines employed in *in vitro* experiments

compared with isotype control mAb (negative controls, empty peak). The fluorescence shifts reported for Jurkat E6.1, EoL-1 and HMC 1.1 cells confirmed that these cell lines strongly express α_4 integrin on their surface, while all other cell lines do not express α4 integrin. A representative result of five independent experiments carried out in triplicate (n = 5) is shown.

Figure S4

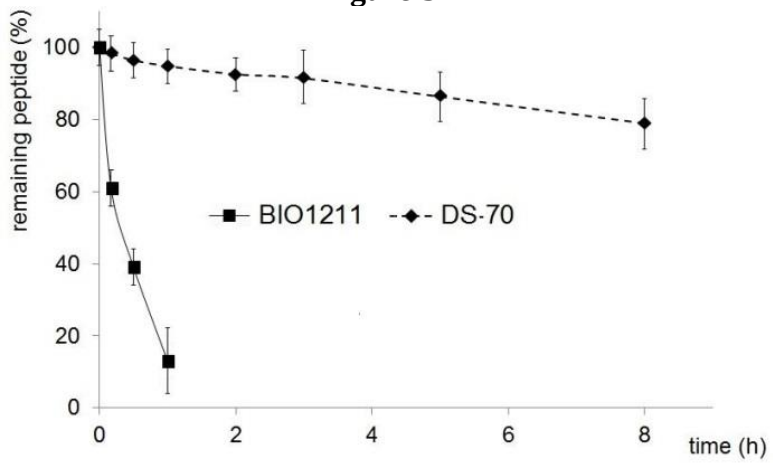

Figure S4

Degradation of BIO1211 and DS-70 in mouse serum. Samples were removed from the incubation solution at 0, 0.15, 0.5, 1.0, 2.0, 4.0, 6.0 and 8.0 h and peptide stability was determined using an RP-HPLC ESI-MS analysis (described in the Methods). Values are presented as mean ± SD (n = 5).

Figure S5

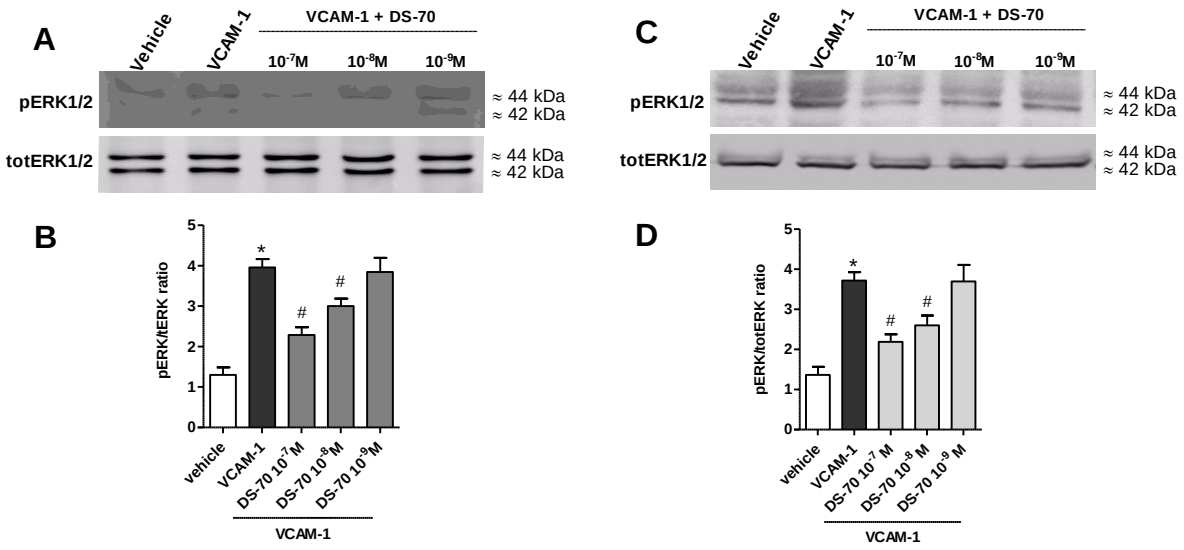

Figure S5

Effects of DS-70 on ERK 1/2 phosphorylation mediated by VCAM-1 in HMC1.1 (A, B) and EoL-1 cells (C, D). (A, C) Representative Western blots confirmed that VCAM-1 is able to induce ERK 1/2 phosphorylation in both cell lines and DS70 maintains its inhibitory effect on this signal transduction pathway. (B, D) The results of semi-quantitative densitometry analysis of the bands from five independent experiments are shown (mean ± SD); the amount of pERK 1/2 is normalized to that of total ERK 1/2. *P < 0.05 *vs.* vehicle; #P < 0.05 *vs.* VCAM-1.

Figure S6

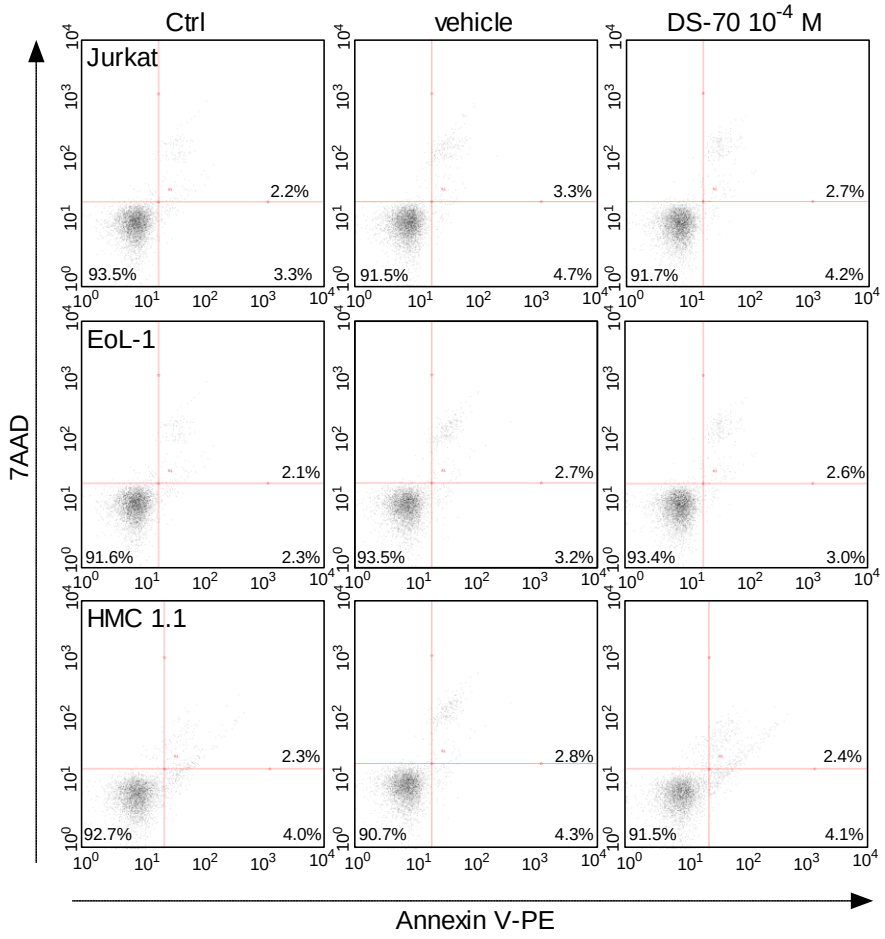

Figure S6

DS-70 does not induce apoptosis in Jurkat E6.1, EoL-1 and HMC1.1 cell lines. Density plots showing the percentage distribution of Jurkat E6.1, HMC 1.1 and EoL-1 control and vehicle or DS-70 (10^{-4} M; 6 h) treated cells. Apoptotic and necrotic cells were quantified by flow cytometry as described in Methods. Non-apoptotic cells (Annexin V and 7-AAD negative) represent 90-95% of the total cell population after treatment. Quadrants: (top left) damaged cells, (top right) late apoptotic/secondary necrotic cells, (lower left) live cells, (lower right) early apoptotic cells. These figures are from a representative experiment carried out at least five times in triplicate.

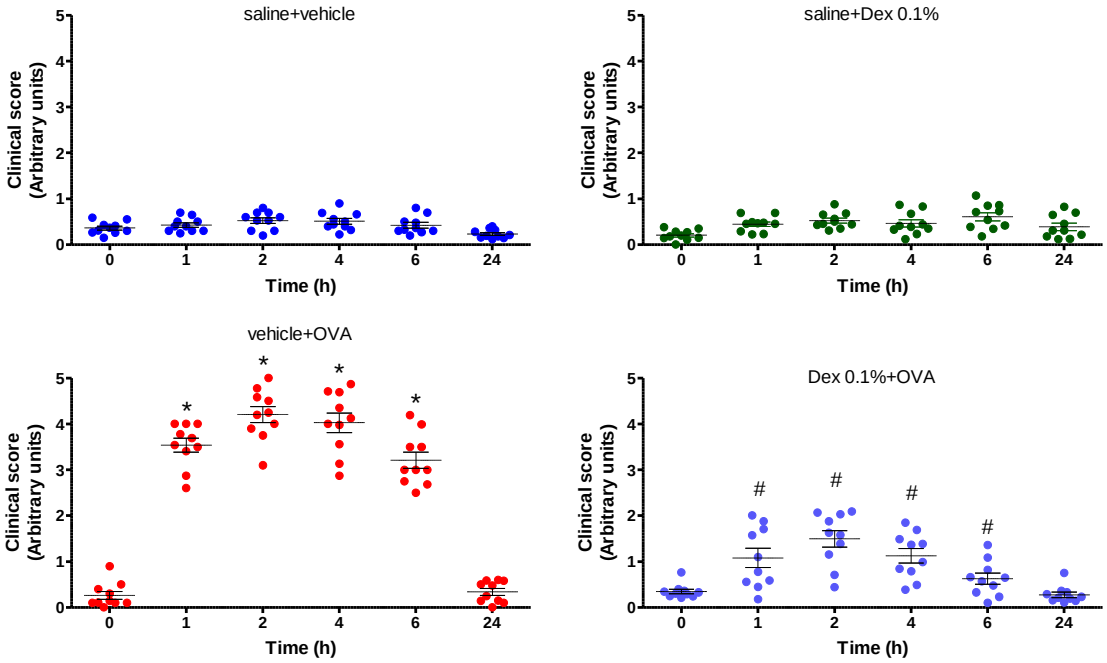

Figure S7

Effects of dexamethasone (Dex) on conjunctival symptoms induced by ovalbumin (OVA) in guinea pigs. Guinea pigs sensitized and challenged with ovalbumin and treated with the vehicle used to dissolve DS-70 (vehicle+OVA) were responsive to the treatment with the consequent increase in clinical score index. Administration of Dex significantly counteracts pathological signs and improves eye appearance. In control guinea pigs sensitized with saline and treated with the vehicle (saline+vehicle) or Dex (saline + Dex 0.1%) no signs of allergic conjunctivitis were observed. Data are presented as scatter plot and refer to the mean ± SD (5 animals per group were included and both eyes were evaluated; n = 10). *$P < 0.05$ *vs*. saline + vehicle; $^{\#}P < 0.05$ *vs*. vehicle + OVA.

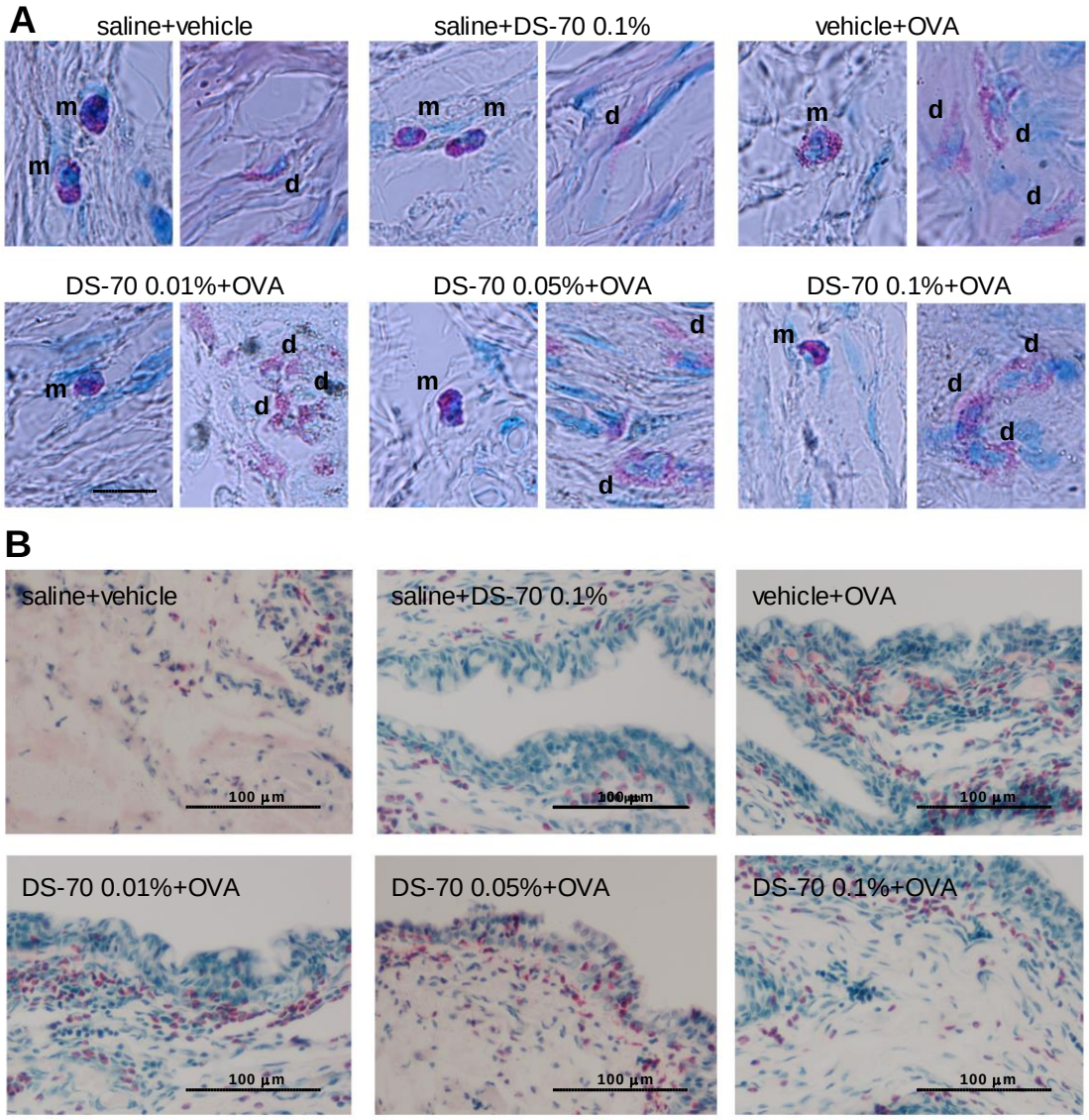

Figure S8

DS-70 prevents, in a dose-dependent manner, conjunctival infiltration and degranulation of mast cells and eosinophils. (A) Histologic analysis of OVA-mediated conjunctival mast cell degranulation. Photomicrographs of tarsal conjunctiva stained with May-Grünwald-Giemsa. Both metachromatic (m) and degranulated (d) mast cells are shown. Black bar = 25 µm. (B) Substantial eosinophil infiltration (Luna's staining) is observed in OVA-treated guinea pigs (vehicle+OVA) in comparison to animals sensitized with saline and treated with the vehicle used to dissolve DS-70 (saline+vehicle) and to animals sensitized with saline and treated with DS-70 alone (saline+DS-70 0.1%) (5 animals per group were included and both eyes were evaluated; n = 10). Scale bar = 100 µm.

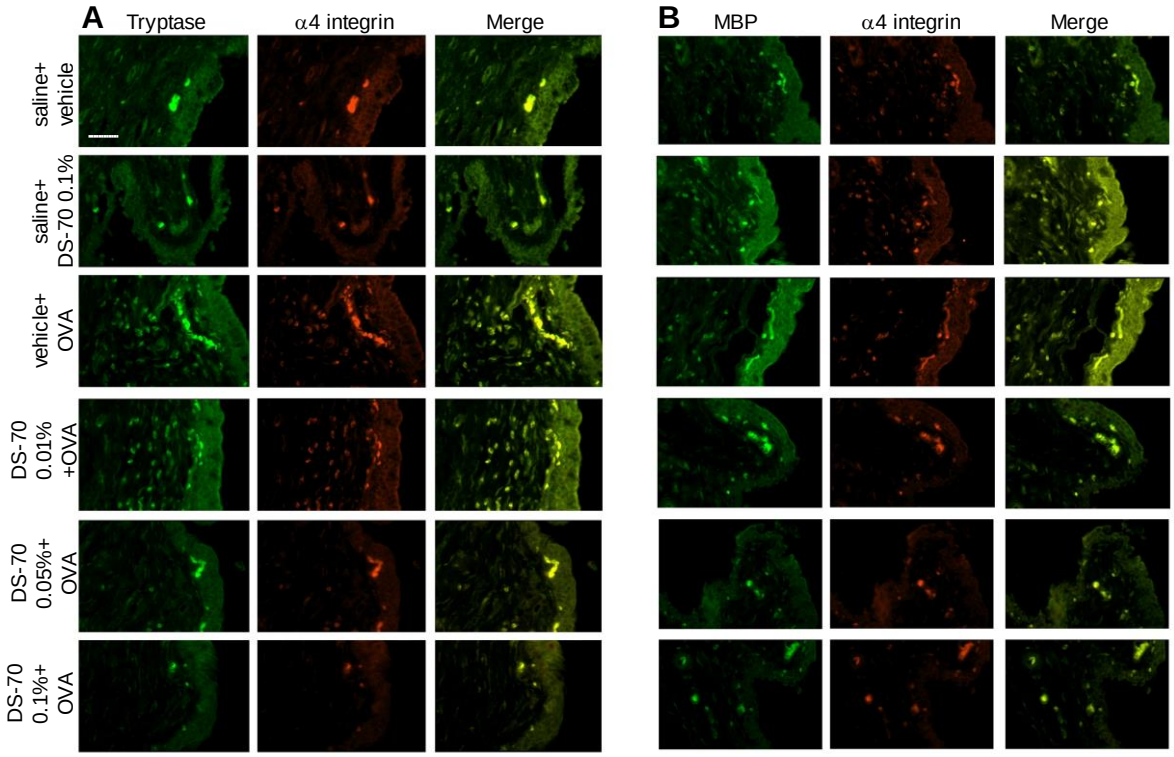

Figure S9

Co-localization of mast cell tryptase or MBP (major basic protein), markers for mast cells and eosinophils respectively, with α_4 integrin in conjunctival sections of guinea pigs sensitized and challenged with ovalbumin and treated with DS-70. (A) Mast cell tryptase and α_4 integrin colocalize on mast cells in conjunctival sections of guinea pig. Double immunofluorescence staining images for tryptase (*green*) and α_4 integrin (*red*) are shown. (B) MBP and α_4 integrin colocalize on eosinophils in conjunctival sections of guinea pig. Double immunofluorescence staining images for MBP (*green*) and α_4 integrin (*red*) are shown (5 animals per group were included and both eyes were evaluated; n = 10). Scale bar = 50 μm.

Table S1. Primers employed in real time PCR experiments.

mRNA target	**Sense primer**	**Antisense primer**
GAPDH	5’-CCGGCCAAATACGATGACAT-3’	5’-TGTAGCCCAAGATGCCTTTGAG-3’
CCL11	5’-TCTGCACACTGCACCATGAA-3’	5’-AAGCAGAGACTGTGAGCAGCA-3’
CCL5	5’-CTGGCCCACTGCTTAGCAAT-3’	5’-CCTTGCTTCTTTGCCTTGAAA-3’
IL-1β	5’-CATGAGCTTCGTACAAGGAGAAAG-3’	5’-CAGGTACAGATTCTTCCCCTTGA-3’
IL-8	5’-CCTTGGATTCCCCTTTATTCCT-3’	5’-CGTATGTCCCCATGACATTGTG-3’

Table S2. Cell lines employed in the study; for each cell lines culture medium, integrin mainly expressed and some references are indicated.

Cell line	Cell culture medium	Integrin mainly expressed	References
SK-MEL-24	Eagle's Minimum Essential Medium (Cambrex, Walkersville, MD, USA) supplemented with FBS (10 mL·100 mL^{-1}; Life technologies, Carlsbad, CA, USA), nonessential amino acids, and sodium pyruvate	$\alpha_v\beta_3$	Baiula et al., 2016; Galletti et al., 2014; Tolomelli et al., 2015
K562	RPMI-1640 medium (Life Technologies), supplemented with 2 mM glutamine and FBS (10 mL·100 mL^{-1})	$\alpha_5\beta_1$	Baiula et al., 2016; Galletti et al., 2014; Tolomelli et al., 2015
Jurkat E6.1		$\alpha_4\beta_1$ and $\alpha_L\beta_2$	see Figure S3; Baiula et al., 2016; Tolomelli et al., 2015; Qasem et al., 2008
EoL-1		$\alpha_4\beta_1$	see Figure S3; Qasem et al., 2008
HEL		$\alpha_{IIb}\beta_3$	Baiula et al., 2016
MCF7		$\alpha_v\beta_5$	Baiula et al., 2016
HT-29		$\alpha_v\beta_6$	Baiula et la., 2016
HL-60		$\alpha_M\beta_2$	Mukai et al., 2017
D283	DMEM (Gibco, LifeTechnologies, Carlsbad, USA) by adding FBS (20 mL·100 mL^{-1}) and non-essential amino acids (Gibco) (1 mL·100 mL^{-1})	$\alpha_9\beta_1$	Fiorilli et al., 2008
RPMI 8866	RPMI-1640 enriched with FBS (10 mL·100 mL^{-1}), 5 mM Hepes and 0.5 mM sodium pyruvate	$\alpha_4\beta_7$	Erle et al, 1994; Tolomelli et al., 2015
HMC 1.1	IMDM medium (Sigma-Aldrich)	$\alpha_4\beta_1$	see Figure S3; Schoeler

	with 25 mM Hepes, supplemented with sodium carbonate (3.02 $g \cdot L^{-1}$), 2 mM glutamine, 1.2 mM α-thioglycerol and FBS (10 $mL \cdot 100\ mL^{-1}$)		et al., 2006

References

Baiula M, Galletti P, Martelli G, Soldati R, Belvisi L, Civera M, et al. (2016). New β-Lactam derivatives modulate cell adhesion and signaling mediated by RGD-binding and leukocyte integrins. J Med Chem 59: 9721-9742.

Erle DJ, Briskin MJ, Butcher EC, Garcia-Pardo A, Lazarovits AI, Tidswell M (1994). Expression and function of the MAdCAM-1 receptor, integrin $alpha_4$ $beta_7$, on human leukocytes. J Immunol. 153: 517-528.

Fiorilli P, Partridge D, Staniszewska I, Wang JY, Grabacka M, So K, *et al*. (2008). Integrins mediate adhesion of medulloblastoma cells to tenascin and activate pathways associated with survival and proliferation. Lab Invest 88: 1143-1156.

Galletti P, Soldati R, Pori M, Durso M, Tolomelli A, Gentilucci L, *et al.* (2014). Targeting integrins αvβ3 and α5β1 with new β-lactam derivatives. Eur J Med Chem 83:284-93.

Mukai M, Suruga N, Saeki N, Ogawa K. (2017) EphA receptors and ephrin-A ligands are upregulated by monocytic differentiation/maturation and promote cell adhesion and protrusion formation in HL60 monocytes. BMC Cell Biol. 18(1):28.

Qasem AR, Bucolo C, Baiula M, Spartà A, Govoni P, Bedini A, et al. (2008) Contribution of alpha4beta1 integrin to the antiallergic effect of levocabastine. Biochem Pharmacol. 76(6):751-62.

Schoeler D, Grützkau A, Henz BM, Küchler J, Krüger-Krasagakis S. (2003) Interleukin-6 enhances whereas tumor necrosis factor alpha and interferons inhibit integrin expression and adhesion of human mast cells to extracellular matrix proteins. J Invest Dermatol. 120(5):795-801.

Tolomelli A, Baiula M, Viola A, Ferrazzano L, Gentilucci L, Dattoli SD, *et al.* (2015) Dehydro-β-proline Containing α4β1 Integrin Antagonists: Stereochemical Recognition in Ligand-Receptor Interplay. ACS Med Chem Lett. 6(6):701-6.